JOC Article

Conformational Analysis of Furanose Rings with PSEUROT: Parametrization for Rings Possessing the Arabino, Lyxo, Ribo, and Xylo Stereochemistry and Application to Arabinofuranosides

Justin B. Houseknecht,[†] Cornelis Altona,[‡] Christopher M. Hadad,[†] and Todd L. Lowary*,[†]

Department of Chemistry, The Ohio State University, 100 West 18th Avenue, Columbus, Ohio 43210, and Leiden Institute of Chemistry, Gorlaeus Laboratories, Leiden University, Box 9502, NL 2300 RA, The Netherlands

lowary.2@osu.edu

Received February 20, 2002

The solution conformation of a furanose ring can be assessed through PSEUROT analysis of three-bond $^1H-^1H$ coupling constants ($^3J_{HH}$) of the ring hydrogens. For each coupling constant, PSEUROT requires two parameters, *A* and *B*, which are used to translate the H−C−C−H dihedral angle predicted from the $^3J_{HH}$ into an endocyclic torsion angle from which the identity of the conformers can be determined. In this paper, we have used density functional theory methods to generate a family of envelope conformers for methyl furanosides **1**−**8**. From these structures, *A* and *B* were calculated for each H−C−C−H fragment. In turn, the values of these parameters for the arabinofuranose ring were used in PSEUROT calculations to determine the conformers populated by monosaccharides **1** and **2** as well as the furanose rings in oligosaccharides **9**−**15**. The results of these analyses are consistent with the low-energy conformers identified from previous computational and X-ray crystallographic studies of **1** and **2**.

Introduction

A standard method for assessing the solution conformation of a furanose ring involves the measurement of the three-bond $^1H-^1H$ coupling constants ($^3J_{HH}$) of the ring hydrogens and subsequent analysis of these data with the program PSEUROT.[1] This program assumes a model in which two conformers are present, one in the northern hemisphere of the pseudorotational wheel (Figure 1), the other in the southern hemisphere. These conformers, termed North (N) or South (S), equilibrate via pseudorotation,[2,3] and each can be described by two coordinates: the Altona−Sundaralingam (AS) pseudorotational phase angle (*P*) and the AS puckering amplitude (ϕ_m).[4,5] With a knowledge of the five endocyclic torsion angles of a given conformer ($\phi_0-\phi_4$, Figure 2), *P* can be calculated through the use of eq 1.[4] The puckering amplitude ϕ_m is related to *P* and ϕ_0 through eq 2.[4]

$$\tan P = \frac{(\phi_2 + \phi_4) - (\phi_1 + \phi_3)}{3.077\phi_0} \quad (1)$$

$$\phi_m = \frac{\phi_0}{\cos P} \quad (2)$$

PSEUROT analysis provides the identities of the two conformers (and their populations) that best fit the experimental $^3J_{HH}$ data. This is done by the correlation of the coupling constants, through a generalized Karplus equation,[6,7] with exocyclic H−C−C−H dihedral angles (ϕ_j^{HH}). In turn, these exocyclic torsion angles must be related to the corresponding endocyclic torsion angles (ϕ_j) from which *P* is calculated. The correlation of ϕ_j^{HH} with ϕ_j is done via eq 3.

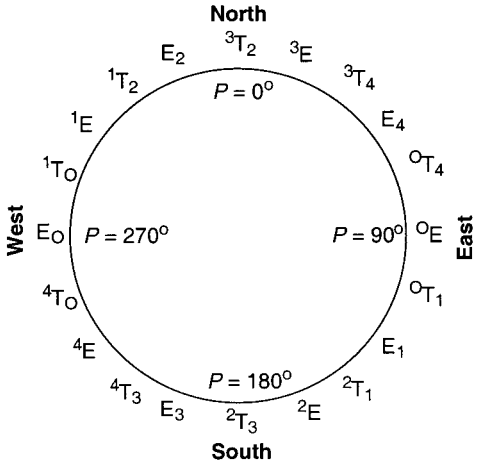

FIGURE 1. Pseudorotational itinerary for a D-aldofuranose ring.

[†] The Ohio State University.
[‡] Leiden Institute of Chemistry.

(1) (a) van Wijk, J.; Haasnoot, C. A. G.; de Leeuw, F. A. A. M.; Huckriede, B. D.; Westra Hoekzema, A.; Altona, C. *PSEUROT 6.2 1993, PSEUROT 6.3 1999*; Leiden Institute of Chemistry, Leiden University. (b) de Leeuw, F. A. A. M.; Altona, C. *J. Comput. Chem.* **1983**, *4*, 428. (c) Altona, C. *Recl. Trav. Chem. Pays-Bas* **1982**, *101*, 413.
(2) Kilpatrick, J. E.; Pitzer, K. S.; Spitzer, R. *J. Am. Chem. Soc.* **1947**, *69*, 2483.
(3) Pitzer, K. S.; Donath, W. F. *J. Am. Chem. Soc.* **1959**, *81*, 3213.
(4) Altona, C.; Sundaralingam, M. *J. Am. Chem. Soc.* **1972**, *94*, 8205.
(5) Altona, C.; Sundaralingam, M. *J. Am. Chem. Soc.* **1973**, *95*, 2333.

10.1021/jo025635q CCC: $22.00
Published on Web 06/13/2002

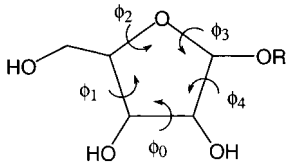

FIGURE 2. Definition of endocyclic torsion angles $\phi_0-\phi_4$. Note that the numbering system originally proposed by Altona and Sundaralingam (ref 4) is used rather than that adopted by the IUPAC−IUB Nomenclature Commission (*Eur. J. Biochem.* **1983**, *131*, 9).

$$\phi_j^{HH} = A_j\phi_j + B_j \quad j = 0, 1, 2, 3, 4 \qquad (3)$$

In the ideal case (Figure 3), where tetrahedral bond angles imply trigonal projection symmetry, A_j and B_j for cis hydrogens will be 1 and 0°, respectively. Similarly, under ideal circumstances, $A_j = 1$ and $B_j = 120°$ for trans hydrogens. However, in rings for which these criteria are not met (e.g., a furanose ring), deviations from these ideal values are observed, and these differences must be considered in the analysis. The constants A_j and B_j can be derived either from the analysis of crystal structure data[8] or, when an insufficient amount of such data is available, from structures calculated by ab initio[9] or density functional theory[10] (DFT) methods.[11−14] A third, less desirable, approach is to approximate these numbers from structurally related systems.[15,16]

In the initial parametrization of PSEUROT, these constants were determined for β-ribofuranosyl and 2-deoxy-β-ribofuranosyl rings through the analysis of a database[8] containing the crystal structures of 178 nucleosides and nucleotides. Using these values, estimates of A_j and B_j for other ring systems (e.g., β-arabinofuranosyl systems) were made,[15] and these values are included in the current version of PSEUROT. More recently, computational methods have been used to determine these constants for other ring systems including carbacyclic nucleosides,[11] 1,4-anhydroalditols,[12] 4-thionucleosides,[13] and carbasugar analogues of methyl arabinofuranosides.[14] However, accurate values of A_j and B_j for furanose rings possessing the arabino, lyxo, xylo, and α-ribo stereochemistry have not been reported. For these compounds, a computational approach is necessary given the paucity of crystallographic data that is available for furanose rings with these configurations.[17−20]

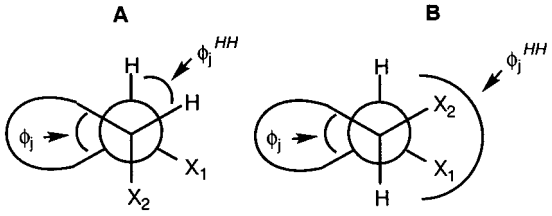

FIGURE 3. Newman projections showing relationship between ϕ_j and ϕ_j^{HH} when all bond angles are tetrahedral. X_1, X_2 = substituent. (A) For cis hydrogens. (B) For trans hydrogens.

CHART 1

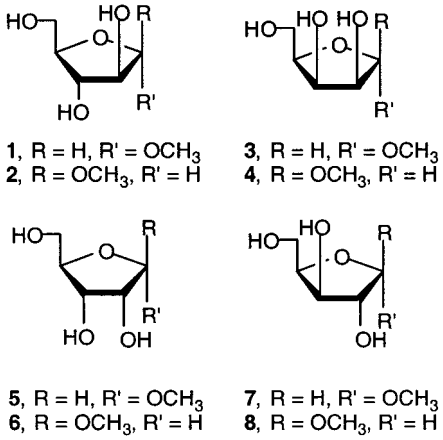

In this paper, we report the use of DFT methods to generate a family of envelope conformers of the methyl furanosides of D-arabinose, D-lyxose, D-ribose, and D-xylose (**1**−**8**, Chart 1). These structures were then used to determine the values of *A* and *B* for each relevant endocyclic torsion angle (angles ϕ_0, ϕ_1, and ϕ_4, Figure 2). Furthermore, armed with these accurate A_j and B_j values, we have carried out PSEUROT analyses on **1** and **2** as well as for each ring in oligosaccharides **9**−**15** (Chart 2) to determine the conformers populated by the furanose rings in these glycans.

Methods

Computational Methods. All DFT calculations were performed using Gaussian 98.[21] For each ring system **1**−**8**, three series of 10 idealized envelope geometries (a total of 30 structures) were constructed differing only in the orientation about the C_4-C_5 bond. In one series, the orientation of this C_4-C_5 bond was gg, another gt, and the third tg (Figure 4A). In all conformers, the dihedral angle about the C_1-O_1 bond was initially chosen to maximize the exo-anomeric effect;[22] i.e., the methyl group was placed antiperiplanar to C_2. The orientations of the hydroxyl hydrogens were initially set as follows: OH_2 anti to C_3, OH_3 anti to C_4, and OH_5 anti to C_4 (Figure 4B). Each conformer was then optimized at the B3LYP/

(6) (a) Haasnoot, C. A. G.; de Leeuw, F. A. A. M.; Altona, C. *Tetrahedron* **1980**, *36*, 2783. (b) Haasnoot, C. A. G.; de Leeuw, F. A. A. M.; de Leeuw, H. P. M.; Altona, C. *Org. Magn. Reson.* **1981**, *15*, 43.
(7) (a) Altona, C.; Francke, R.; de Haan, R.; Ippel, J. H.; Daalmans, G. J.; Westra Hoekzema, A. J. A.; van Wijk, J. *Magn. Reson. Chem.* **1994**, *32*, 670. (b) van Wijk, J.; Huckriede, B. D.; Ippel, J. H.; Altona, C. *Methods Enzymol.* **1992**, *211*, 286.
(8) De Leeuw, H. P. M.; Haasnoot, C. A. G.; Altona, C. *Isr. J. Chem.* **1980**, *20*, 108.
(9) Hehre, W. J.; Radom, L.; Schleyer, P. v. R.; Pople, J. A. *Ab Initio Molecular Orbital Theory*; John Wiley & Sons: New York, 1986.
(10) (a) Labanowski, J. W.; Andzelm, J. *Density Functional Methods in Chemistry*; Springer: New York, 1991. (b) Parr, R. G.; Yang, W. *Density Functional Theory in Atoms and Molecules*; Oxford University Press: New York, 1989.
(11) Thibaudeau, C.; Kumar, A.; Bekiroglu, S.; Matsuda, A.; Marquez, V. E. Chattopadhyaya, J. *J. Org. Chem.* **1998**, *63*, 5447.
(12) Plavec, J.; Tong, W.; Chattopadhyaya, J. *J. Am. Chem. Soc.* **1993**, *115*, 9734.
(13) Crnugelj, M.; Dukhan, D.; Barascut, J.-L.; Imbach, J.-L.; Plavec, J. *J. Chem. Soc., Perkin Trans. 2* **2000**, 255.
(14) Callam, C. S.; Lowary, T. L. *J. Org. Chem.* **2001**, *66*, 8961.
(15) De Leeuw, F. A. A. M.; Altona, C. *J. Chem. Soc., Perkin Trans. 2.* **1982**, 375.
(16) Hoffman, R. A.; van Wijk, J.; Leeflang, B. R.; Kamerling, J. P.; Altona, C.; Vliegenthart, J. F. G. *J. Am. Chem. Soc.* **1992**, *114*, 3710.
(17) Groth, P.; Hammer, H. *Acta Chem. Scand.* **1968**, *22*, 2059.
(18) Podlasek, C. A.; Stripe, W. A.; Carmichael, O.; Shang, M.; Basu, B.; Serianni, A. S. *J. Am. Chem. Soc.* **1996**, *118*, 1413.
(19) Evdokimov, A. G.; Kalb, A. J.; Koetzle, T. F.; Klooster, W. T.; Martin, J. M. L. *J. Phys. Chem. A* **1999**, *103*, 744.
(20) Evdokimov, A.; Gilboa, A. J.; Koetzle, T. F.; Klooster, W. T.; Schultz, A. J.; Mason, S. A.; Albinati, A.; Frolow, F. *Acta Crystallogr. B* **2001**, *57*, 213.

CHART 2

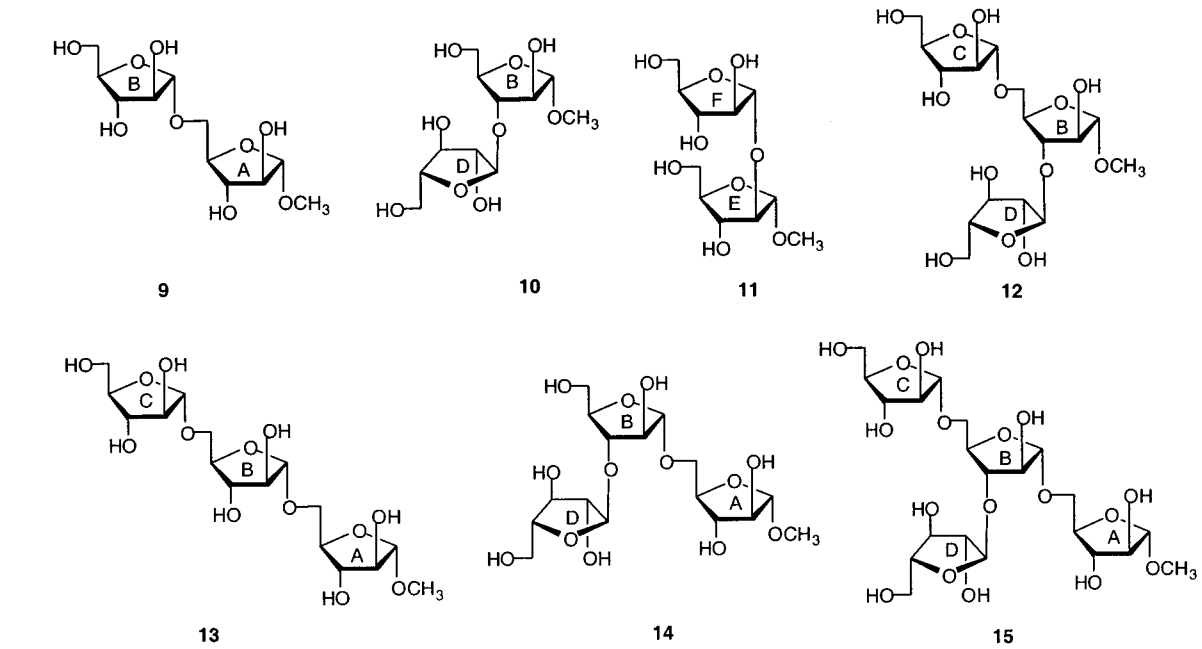

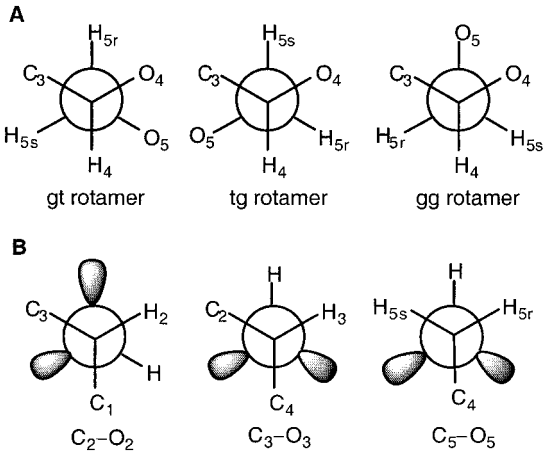

FIGURE 4. (A) Definition of gg, gt, and tg rotamers about the C_4-C_5 bond. (B) Initial orientations about the C−O bonds.

6-31G* level of theory.[23] In these optimizations, one endocyclic dihedral angle was fixed in a plane to maintain the envelope conformation (e.g., for an ^{0}E conformer, the $C_1-C_2-C_3-C_4$ dihedral angle was constrained at 0°). All other geometric parameters (bond distances, bond angles, and dihedral angles) were allowed to optimize completely. The orientation about the exocyclic C−O bonds for some conformers changed upon optimization. These changes were generally to a position more favorable for the formation of intramolecular hydrogen bonds. For the C_1-O_1 or C_4-C_5 bonds, no substantial rotameric changes were observed. However, slight deviations away from the initial ideally staggered orientation were sometimes observed. All of the gas-phase geometries of **1**−**8** were, in turn, further optimized in an aqueous model for solvation[24] at the SM5.42/BPW91/6-31G* level of theory[25] with the planar constraint in place. This procedure provided 30 aqueous-phase conformers each of **1**−**8**.

Determination of A and B. With all of the gas-phase and aqueous-phase conformers in hand, the ϕ_0, ϕ_1, and ϕ_4 values were extracted as were all ϕ_j^{HH} values. Tables containing these data are provided in the Supporting Information (Tables S1−S16). Subsequently, for a given family of conformers (e.g., the 30 gas-phase envelope conformers of **1**), three graphs were generated. In each, one ϕ_j was plotted against the appropriate ϕ_j^{HH}; e.g., ϕ_1 was plotted against the $H_3-C_3-C_4-H_4$ torsion angle. These plots are included in the Supporting Information, and in each, these data were fit to a straight line with the slope being *A* and the *y*-intercept being *B* for that H−C−C−H fragment. There was an excellent fit of the data to a straight line, with $R^2 > 0.993$ in all cases.

PSEUROT Calculations. The coupling constants used in the PSEUROT calculations of **1**, **2**, and **9**−**15** have previously been reported.[26,27] In all calculations, the ϕ_m was kept constant at 39° as this corresponds to the puckering amplitude of the ring in the crystal structures of **1** and **2**. The values of *A* and *B* used were those calculated from the aqueous-phase geometries (Table 1), and the electronegativities of the substituents

(21) Frisch, M. J.; Trucks, G. W.; Schlegel, H. B.; Scuseria, G. E.; Robb, M. A.; Cheeseman, J. R.; Zakrzewski, V. G.; Montgomery, J. A., Jr.; Stratmann, R. E.; Burant, J. C.; Dapprich, S.; Millam, J. M.; Daniels, A. D.; Kudin, K. N.; Strain, M. C.; Farkas, O.; Tomasi, J.; Barone, V.; Cossi, M.; Cammi, R.; Mennucci, B.; Pomelli, C.; Adamo, C.; Clifford, S.; Ochterski, J.; Petersson, G. A.; Ayala, P. Y.; Cui, Q.; Morokuma, K.; Malick, D. K.; Rabuck, A. D.; Raghavachari, K.; Foresman, J. B.; Cioslowski, J.; Ortiz, J. V.; Stefanov, B. B.; Liu, G.; Liashenko, A.; Piskorz, P.; Komaromi, I.; Gomperts, R.; Martin, R. L.; Fox, D. J.; Keith, T.; Al-Laham, M. A.; Peng, C. Y.; Nanayakkara, A.; Gonzalez, C.; Challacombe, M.; Gill, P. M. W.; Johnson, B.; Chen, W.; Wong, M. W.; Andres, J. L.; Gonzalez, C.; Head-Gordon, M.; Replogle, E. S.; Pople, J. A. *Gaussian 98*, revision A.9; Gaussian, Inc.; Pittsburgh, PA, 1998.

(22) Lemieux, R. U.; Koto, S. *Tetrahedron* **1974**, *30*, 1933.

(23) (a) Becke, A. D. *Phys. Rev. A* **1988**, *38*, 3098. (b) Becke, A. D. *J. Chem. Phys.* **1993**, *98*, 5648. (c) Lee, C.; Yang, W.; Parr, R. G. *Phys. Rev. B* **1988**, *37*, 785.

(24) Cramer, C. J.; Truhlar, D. G. *Chem. Rev.* **1999**, *99*, 2161.

(25) (a) Xidos, J. D.; Li, J.; Hawkins, G. D.; Liotard, D. A.; Cramer, C. J.; Truhlar, D. G.; Frisch, M. J. *MN-GSM*, version 99.2; University of Minnesota: Minneapolis, MN, 555455. (b) Li, J.; Zhu, T.; Cramer, C. J.; Truhlar, D. G. *J. Phys. Chem. A* **1998**, *102*, 1820. (c) Li, J.; Hawkins, G. D.; Cramer, C. J.; Truhlar, D. G. *Chem. Phys. Lett.* **1998**, *288*, 293. (d) Zhu, T.; Li, J.; Hawkins, G. D.; Cramer, C. J.; Truhlar, D. G. J. *Chem. Phys.* **1998**, *109*, 9117. (e) Li, J.; Zhu, T.; Hawkins, G. D.; Winget, P.; Liotard, D. A.; Cramer, C. J.; Truhlar, D. G. *Theor. Chem. Acc.* **1999**, *103*, 9.

(26) D′Souza, F. W.; Ayers, J. D.; McCarren, P. R.; Lowary, T. L. *J. Am. Chem. Soc.* **2000**, *122*, 1251.

(27) Gordon, M. T.; Lowary, T. L.; Hadad, C. M. *J. Org. Chem.* **2000**, *65*, 4954.

TABLE 1. Values of *A* and *B* for the ϕ_0, ϕ_1, and ϕ_4 Endocyclic Torsion Angles in 1−8[a]

		ϕ_4 (C_1-C_2 bond)[b]		ϕ_0 (C_2-C_3 bond)[b]		ϕ_1 (C_3-C_4 bond)[b]	
compd	phase	*A*	*B*[c]	*A*	*B*[c]	*A*	*B*[c]
1	gas	1.06	−125.4	1.15	125.8	1.04	−126.4
1	aqueous	1.03	−126.5	1.14	126.6	1.03	−127.4
1	PSEUROT	1.10	−116.7	1.09	120.2	1.10	−124.9
2	gas	1.07	−2.4	1.12	124.9	1.03	−126.4
2	aqueous	1.07	−2.0	1.12	125.9	1.02	−127.3
2	PSEUROT	1.10	3.3	1.09	120.2	1.10	−124.9
3	gas	1.05	−123.0	1.13	−0.1	1.04	−1.6
3	aqueous	1.03	−123.6	1.13	−0.4	1.03	−2.0
3	PSEUROT	1.10	−116.7	1.09	0.2	1.10	−4.9
4	gas	1.06	0.4	1.12	−1.1	1.02	−2.3
4	aqueous	1.05	0.8	1.10	−1.3	1.01	−2.3
4	PSEUROT	1.10	3.3	1.09	0.2	1.10	−4.9
5	gas	1.05	−0.2	1.14	0.9	1.03	−124.8
5	aqueous	1.03	−0.5	1.12	0.8	1.02	−125.3
5	PSEUROT	1.10	3.3	1.09	0.2	1.10	−124.9
6	gas	1.05	123.2	1.17	−0.4	1.04	−125.1
6	aqueous	1.03	123.8	1.15	−0.6	1.04	−125.2
6	PSEUROT	1.10	123.3	1.09	0.2	1.10	−124.9
7	gas	1.07	2.4	1.11	−125.4	1.03	−0.5
7	aqueous	1.06	2.2	1.10	−126.4	1.04	−0.6
7	PSEUROT	1.10	3.3	1.09	−119.8	1.10	−4.9
8	gas	1.06	125.2	1.13	−126.3	1.04	−0.3
8	aqueous	1.04	126.3	1.13	−126.9	1.04	−0.3
8	PSEUROT	1.10	123.3	1.09	−119.8	1.10	−4.9

[a] See the Methods and Supporting Information for details on how these values were calculated. [b] See Figure 2 for torsion angle definitions. [c] In degrees.

TABLE 2. PSEUROT Analysis of 1, 2, and 9−15[a,b]

compd	ring[c]	P_N[d] (deg)	N conformer[e]	X_N (%)	P_S[d] (deg)	S conformer[e]	X_S (%)	rms (Hz)
1		46	$^3T_4/E_4$	44	130	E_1	56	0.0
2		351	$^3T_2/E_2$	89	193	E_3	11	0.0
9	A	45	$^3T_4/E_4$	40	126	E_1	60	0.0
	B	44	$^3T_4/E_4$	39	121	$^0T_1/E_1$	61	0.0
10	B	42	$^3T_4$	26	120	$^0T_1/E_1$	74	0.0
	D	48	$^3T_4/E_4$	46	125	E_1	54	0.0
11	E[f]	54	E_4	49	130	E_1	51	0.0
	F	61	$E_4/^0T_4$	56	137	$E_1/^2T_1$	44	0.0
12	B	53	E_4	28	124	E_1	72	0.0
	C	48	$^3T_4/E_4$	44	128	E_1	56	0.0
	D	49	$^3T_4/E_4$	46	129	E_1	54	0.0
13	A	43	$^3T_4$	40	125	E_1	60	0.0
	B	46	$^3T_4/E_4$	42	125	E_1	58	0.0
	C	48	$^3T_4/E_4$	44	128	E_1	56	0.0
14	A	46	$^3T_4/E_4$	43	136	$E_1/^2T_1$	57	0.0
	B	45	$^3T_4/E_4$	26	117	$^0T_1/E_1$	74	0.0
	D	48	$^3T_4/E_4$	46	125	E_1	54	0.0
15	A	42	$^3T_4$	42	127	E_1	58	0.0
	B	42	$^3T_4$	23	118	$^0T_1/E_1$	77	0.0
	C	48	$^3T_4/E_4$	44	130	E_1	56	0.0
	D	48	$^3T_4/E_4$	44	127	E_1	56	0.0

[a] Calculated using a constant $\phi_m = 39$. [b] The analysis was carried out using the A_j and B_j values determined from aqueous-phase conformers. [c] See Chart 2 for assignment of ring letters. [d] P = pseudorotational phase angle. [e] See Figure 1 for conformer definitions. [f] Coupling constants from ring E were obtained from the ^{1}H NMR spectrum simulated by NMRSim (Bruker).

employed were as follows: 1.25 for OH; 1.26 for OR; 0.68 for CH_2OH; 0.50 for $CH(OR)_2$; 0.0 for H.[7] The results of these PSEUROT calculations are provided in Table 2. Another series of calculations was done in which the ϕ_m was kept constant at 35° (see Table S18 for results).

Results and Discussion

To calculate A_j and B_j values for **1**−**8**, it was first necessary to generate a large number of envelope conformers for these ring systems, from which the appropriate dihedral angles could be extracted. These starting structures were built as described above, and B3LYP/6-31G* optimization afforded a total of 30 gas-phase envelope conformers for each ring system. Given that most NMR studies of furanose rings are carried out in water, we viewed it important to investigate the effect of aqueous solvation on these torsion angles. Accordingly, each of the gas-phase structures was then reoptimized using the MN-GSM solvation model,[25] which yielded 30 aqueous-phase envelope conformers for **1**−**8**. We have previously demonstrated the success of the MN-GSM solvation model in treating carbohydrates[28] and glycerol.[29]

Using the methods outlined above, the *A* and *B* values for the ϕ_0, ϕ_1, and ϕ_4 endocyclic torsions in **1**−**8** were calculated; these data are provided in Table 1. For purposes of comparison, the default values available in the current version of the PSEUROT program are also included. It is clear that the A_j and B_j calculated from the gas-phase geometries are quite similar to those calculated from the aqueous geometries. However, when these values are compared to those currently available in PSEUROT, larger differences are observed. In particular, the magnitude of B_j differs substantially in many cases. Overall, the best agreement between the default A_j and B_j values and those calculated here is seen with the β-ribose case (**6**). This is to be expected given that PSEUROT was initially parametrized using crystal structure data consisting, in large part, of β-ribofuranosyl-containing nucleotides. It appears, therefore, that the anomeric *O*-methyl group can be interchanged for a nucleoside base without significant effect on either A_j or B_j.

The availability of more accurate A_j and B_j for the arabinofuranose ring (**1** and **2**) enabled PSEUROT analysis of the $^3J_{HH}$ of **1**, **2**, and **9**−**15** (Chart 2) measured from spectra taken of samples dissolved in D_2O. Shown in Table 2 are the results of these analyses using the A_j and B_j values calculated from the aqueous-phase conformers of **1** and **2**. An analogous series of calculations was carried out using the A_j and B_j values calculated from the gas-phase conformers. Only small differences in conformer identity and population were observed between the two series of calculations. The results of the PSEUROT analyses using the gas-phase A_j and B_j values are included in the Supporting Information (Table S17).

In all cases, the use of these new values of *A* and *B* provided results with excellent rms errors in comparison with those previously reported by us.[26,27,30] Moreover, the results of these calculations, particularly for **1** and **9**−**15**, differ significantly from those previously determined,[26] thus underscoring the importance of the improved A_j and B_j parameters used in these calculations.

For monosaccharide **1**, the ring exists as an essentially equimolar N/S mixture of $^3T_4/E_4$ (N) and E_1 (S) conformers. These results compare very well with our previous

(28) Houseknecht, J. B.; McCarren, P. R.; Lowary, T. L.; Hadad, C. M. *J. Am. Chem. Soc.* **2001**, *123*, 8811.
(29) Callam, C. S.; Singer, S. J.; Lowary, T. L.; Hadad, C. M. *J. Am. Chem. Soc.* **2001**, *123*, 11743.
(30) In these calculations, we kept the ϕ_m of the rings constant at 39°, which is the puckering amplitude of the rings in the crystal structures of **1** and **2**.

gas-phase calculations on **1**, which identified structures in the $^3E-E_4$ and $^2E-^2T_1$ regions of the pseudorotational wheel (Figure 1) as the low energy conformers.[31] Subsequent calculations on **1**, in which solvation was considered, provided similar results.[32] In the crystal structure of **1**, the ring adopts an E_4 conformation,[19,20] close to the N aqueous-solution minimum. In the case of **2**, the PSEUROT calculations predict an equilibrium heavily biased toward a N structure that is intermediate between the idealized $^3T_2$ and E_2 conformers. Here again, these results compare favorably with previous gas-phase calculations[27] on **2** as well as the ring conformation in the crystal structure, which is $^1T_2$.[20]

In oligosaccharides **9**−**15**, the conformers populated by the rings differ only slightly from those present in **1**. For all of these rings, *P* varies by only ±20°. The most noticeable trend is that the N/S ratio of the 3-*O*-substituted rings (ring B in **10**, **12**, **14**, and **15**) is biased toward the S conformer. The N/S ratio of these residues is ∼1:3 compared to ∼1:1 in the monosaccharide parent. In contrast, glycosylation of the other secondary hydroxyl group (OH_2) does not have the same effect; the N/S ratio of ring E in **11** is 1:1.

The rms errors in all of these calculations are excellent. However, it should be appreciated that for the arabinofuranose ring only three coupling constants are available ($^3J_{1,2}$, $^3J_{2,3}$, and $^3J_{3,4}$). Because five parameters are required to describe the system (the *P* and ϕ_m of both conformers and the percentage of one of them), the system is underdetermined. As is standard in these analyses,[1] this problem was addressed by fixing the ϕ_m of both conformers to 39°, which corresponds to the puckering amplitude of the ring present in the crystal structure in **1** and **2**. We also carried another series of PSUEROT calculations in which the ϕ_m of both conformers were fixed at 35°, and the results obtained (Table S18) were very similar to those with given in Table 2. In all cases, only small differences in *P* and conformer populations were observed. However, the validity of setting the ϕ_m of both conformers to a single fixed value can be questioned, especially for rings that contain no cis related adjacent substituents (e.g., α-arabino). The puckering amplitude in these rings would be expected to be more variable than in those that contain at least one pair of cis oriented adjacent substituents (e.g., *β*-ribo). More accurate results may therefore be obtained through analysis of additional coupling constant data obtained at a number of temperatures. Such investigations on **1**, **2**, and **9**−**15** are in progress. Furthermore, given the paucity of experimental coupling constant data for methyl furanosides possessing the lyxo, xylo, and α-ribo stereochemistry, application of the *A* and *B* values shown in Table 1 to the analysis of **3**−**8** must await the synthesis of these compounds and subsequent measurement of the appropriate $^3J_{H,H}$. The results of these investigations, which are also currently in progress, will be reported separately.

(31) McCarren, P. R.; Gordon, M. T.; Lowary, T. L.; Hadad, C. M. *J. Phys. Chem. A* **2001**, *105*, 5911.

(32) McCarren, P. R.; Lowary, T. L.; Hadad, C. M. Manuscript in preparation.

Conclusion

In summary, DFT methods have been used to generate a family of conformers for methyl furanosides **1**−**8**. From these structures, key PSEUROT parameters, A_j and B_j, were calculated for each ring system. In turn, the A_j and B_j values for the arabinofuranose ring were used in PSEUROT calculations to determine the conformers populated by monosaccharides **1** and **2** as well as the furanose rings in **9**−**15**. The results of these analyses are consistent with the low-energy conformers identified from previous computational and X-ray crystallographic studies of **1** and **2**.

Acknowledgment. This work was supported by the National Science Foundation (CHE-9875163 and CHE-9733457) and the Ohio Supercomputing Center. J.B.H. is supported as a graduate research fellow by an NIH Training Grant for Chemistry at the Biology Interface. We thank Christopher J. Cramer and Donald G. Truhlar for access to the MN-GSM code at the Minnesota Supercomputing Institute.

Supporting Information Available: Cartesian coordinates for all optimized geometries of **1**−**8**; tables containing all ϕ_j and ϕ_j^{HH} used for calculating A_j and B_j for **1**−**8**; plots of ϕ_j vs ϕ_j^{HH} from which A_j and B_j were determined; tables containing the results of additional PSEUROT calculations on **1**, **2**, and **9**−**15**. This material is available free of charge via the Internet at http://pubs.acs.org.

JO025635Q